A DUAL NORMAL MODE REPRESENTATION FOR ELECTROMAGNETIC SCATTERING: SOME INITIAL CONSIDERATIONS

T. H. Lehman
927 Camino Del Rio NW
Albuquerque, NM 87114

ABSTRACT

This paper presents a new technique for characterizing the electromagnetic interaction with and scattering from objects of finite extent. By exploiting the structure of the operators (in this case matrices) associated with the interaction, it is shown that both the system (impedance) matrix and the transfer (admittance) matrix can be partitioned into the sum of two matrices such that each of the resulting matrices can be decomposed into a set of normal modes. As a result, the number of parameters needed to describe the interaction is now significantly reduced and the parameters identified by this technique are model independent, i.e. they are measurable parameters. Potential applications of the technique include EM computations, compact descriptions of scatterers and antennas, interpretation of measured data, and algorithm development applicable to scattering and inverse scattering problems.

INTRODUCTION

There are a number of numerical methods available for determining the induced currents on or fields scattered from a wide class of objects. Direct applications of all of these methods – which include method of moments, finite element, finite difference, etc. – yield interaction or scattering representations which are exclusively in terms of a large number of abstract parameters (model dependent parameters). Although, in principle, these parameters can be related to the measured or observed parameters (model independent parameters) of the interaction, this usually is very difficult to accomplish when it can be done at all. This disparity between measured and model parameters significantly reduces the utility of these models for most applications to practical problems other than as computational tools for specific cases.

This requirement for an "observable parameter based EM model" is not new and has provided the impetus for considerable research in the area. Two methods resulting from this research are worth noting. The first of these methods is the Eigenmode Expansion Method (EEM) which is simply a re–statement of the fact that a non–normal matrix, say Z, can be diagonalized by a similarity transformation or

$$e = T^{-1}ZT \qquad (1)$$

where the elements of the diagonal matrix e are the eigenvalues of Z, T is the matrix of right eigenvectors and T^{-1}, the inverse of T, is the matrix of left eigenvectors. If Z is the impedance matrix obtained by application of the frequency domain method of moments formulation to an antenna or scatterer, then not only is Z a function of the frequency, f, but in general, e and T are also functions of f (usually complicated and irrational functions). The only real advantage of this formulation is that each eigenvector $(T)_j$ is orthogonal with respect to all other eigenvectors $(T)_k$.

The second method worth noting is the Singularity Expansion Method (SEM) [Baum (1971)]. It is intimately related to the EEM method in that it decomposes Z (the system matrix) or $Y = Z^{-1}$ (the transfer matrix) into a set of time invariant vectors (independent of f or the complex frequency s) and a diagonal matrix representation that contains all of the time or frequency dependence. For the interior problem with only ohmic losses (restricts Z(s) to be second order in s), it is straight–forward but tedious to show [Richardson and Potter (1974)] that each element of the admittance matrix Y can be expanded into a partial fraction expansion about each pole of Z(s) so that Y can be written in the form

$$Y = \sum_{k=1}^{M} A_k/(s-s_k) \quad , \tag{2}$$

where M = 2N, the A_k's are matrices independent of s, and the s_k's are the poles of Z(s). The A_k's are evaluated by setting $s=s_k$ in the following equation

$$A_k = T(s)(s-s_k)e^{-1}(s)T^{-1}(s) \tag{3}$$

where T and e are defined by equation (1). In this formulation, the s_k's are referred to as the complex natural frequencies of the system.

Applications of this methodology to the exterior problem where ohmic losses are replaced by radiation losses significantly increases the complexity of the formulation and its understanding. First of all, the impedance matrix Z is no longer second order in s and is at least of order N [Cordaro and Davis (1981)] where N is the dimensionality of the impedance matrix. There are now on the order of $2N^2$ natural frequencies instead of the 2N natural frequencies associated with the internal problem (the factor of 2 arises because the poles occur in conjugate pairs). Secondly, the mode shapes associated with the natural frequencies are no longer orthogonal or real (this was also true for the interior problem). Lastly, only the first row of the natural frequencies s_{1k} have been observed experimentally. As a consequence, the admittance matrix has been written in the form

$$Y = \sum_{k=1}^{M} A_{1k}/(s-s_{1k}) + \text{"entire function"} \quad . \tag{4}$$

Here the "entire function" somehow accounts for the driven response of the scatterer while the sum over the poles accounts for the undriven response. The functional form of the entire function has yet to be uniquely defined. To date the SEM representation has proven to be too complex and too difficult both theoretically and experimentally to be of much practical value except for a few specific cases. It seems rather obvious that the "entire function" in equation (4) arises because the A_{1k}'s do not form a complete set of natural frequency mode shapes. If all of these mode shapes are required, then the SEM formulation results in replacing one NxN frequency dependent full matrix by N NxN frequency dependent diagonal matrices and N NxN frequency independent full complex matrices. But, "Is this representation simpler than the original matrix?"

The next question is "Where does one go from here?" It appears that the cure is worse than the disease. There are three possible cases. The first is that there are no "measurable parameter based EM models" that are simple and easy to apply. Certainly, the results obtained to date seem to support this argument. The second is that simple and easy to apply "measurable parameter based EM models" do exist but that the theoretical and experimental tools necessary for developing these models currently do not exist. The third is that these models have not been developed primarily because of misconceptions held about the nature and existence of normal modes. It is this last case that is examined in some detail in the remainder of this paper.

We begin by examining the concept of classical normal modes. It is well–known that for a linear phenomenon which obeys the wave equation and for which the interaction takes place within a bounded region of space (an interior problem), the "system response" can be decomposed into an infinite number of normal modes as long as all losses or damping mechanisms are ignored. As the name implies, these modes represent independent degrees of freedom (they are orthogonal to each other) and they are defined to be measurable parameters because they do not depend on the analytical formulation of the problem. If a loss or damping mechanism is now introduced into the interaction, then, in general, the response can no longer be decomposed into normal modes and the modes are no longer independent (although for most problems of interest, orthogonality is a good approximation even for the case of large damping coefficients). As a result, it is generally accepted that normal modes exist only for those interactions for which there is no loss or damping, although it has been shown [Caughey and O'Kelly (1965)] that this is not universally true. It should be noted that for interior problems, damping is directly related to the constitutive parameters of the media; for example, for a cavity problem we have no damping if we assume that the cavity walls are perfectly conducting. For the exterior problem (scattering), we know that radiation damping is always present independent of the nature of the media parameters. Therefore, it is easy to assume that the response of scatterers cannot be decomposed into normal modes, even though a few objects (most notably a circular wire loop and a perfectly conducting sphere) do exhibit normal mode behavior.

The behavior of the circular wire loop and the sphere pose some interesting questions. "Is it an accident of nature that their response can be decomposed into normal modes?" These two objects still radiate, so is there some property of their radiation mechanism that makes them different than say a thin straight wire? Or is it possible that the response of all perfectly conducting scatterers can be decomposed into normal modes and that the wire loop and the sphere are limiting cases of some yet to be determined higher order normal mode theory (i.e. for these geometries the higher order theory reduces to the canonical form of normal mode theory)? We now investigate this possibility.

THE DUAL NORMAL MODE REPRESENTATION OF THE IMPEDANCE MATRIX

Consider a thin straight wire defined by a length 2L, a radius a and an impedance matrix $Z_w(f)$ obtained from discretizing Pocklington's equation with the reduced kernel. We do not have to specify the discretization procedure since the structure of Z_w is form invariant with respect to the method of discretization. In other words, Z_w is a Toeplitz matrix irrespective of how it was obtained. The second attribute of Z_w of note, is that if we evaluate it at two different frequencies, say f_1 and f_2, then the two matrices that result from this calculation, do not commute:

$$[Z_w(f_1), Z_w(f_2)] = Z_w(f_1)Z_w(f_2) - Z_w(f_2)Z_w(f_1) \neq 0$$

unless $f_1 = f_2$. Therefore, we know that $Z_w(f_1)$ and $Z_w(f_2)$ cannot be diagonalized by the same similarity transformation and that "classical" normal mode theory is not applicable to a thin wire scatterer.

Since Z_w does not exhibit normal mode behavior, the next question is "does any part of Z_w exhibit normal mode behavior?" The answer to this question is yes. By carefully examining the structure of Z_w, it can be shown that Z_w can be partitioned into the sum of two matrices (see Appendix A) such that each matrix can be diagonalized by a frequency independent similarity transformation:

$$Z_w(f) = Z_1(f) + Z_2(f) \tag{5}$$

where

$$[Z_1(f_1), Z_1(f_2)] = 0 \tag{6}$$

and

$$[Z_2(f_1), Z_2(f_2)] = 0 \tag{7}$$

for arbitrary f_1 and f_2. Therefore, there exists two time or frequency independent matrices, T_1 and T_2, [Arfken (1966)] such that

$$T_1^t Z_1(f) T_1 = z_1(f) \tag{8}$$

and

$$T_2^t Z_2(f) T_2 = z_2(f) \tag{9}$$

for all values of the frequency, f, where $z_1(f)$ and $z_2(f)$ are diagonal matrices and

$$T_1^t = T_1^{-1} = \text{transpose of } T_1 \tag{10}$$

$$T_2^t = T_2^{-1} = \text{transpose of } T_2. \tag{11}$$

Therefore, both Z_1 and Z_2 are diagonalizable by orthogonal similarity transformations.

Equations (8), (9), (10) and (11) allow us to write the impedance matrix, Z_w, for the thin wire in a very simple and compact form:

$$Z_w(f) = T_1 z_1(f) T_1^t + T_2 z_2(f) T_2^t \quad . \tag{12}$$

Thus Z_w can be expressed in terms of two frequency dependent diagonal matrices and two frequency independent orthogonal matrices. Some of the interesting properties of these matrices are:

(1) The matrix elements of both T_1 and T_2 are real.

(2) The first N/2 columns of T_1 and T_2 represent symmetric mode shapes and the second N/2 columns of T_1 and T_2 represent anti–symmetric mode shapes.

(3) Both T_1 and T_2 form complete sets of eigenvectors; so that the current and the incident field can be expanded in terms of either set.

(4) Both the symmetric $(T_1)_s$ and anti–symmetric $(T_1)_a$ modes of Z_1 are analytic functions of the position, x, along the length of the wire and are of the form

$$(T_1)_s = \cos((2n+1)\,\pi\, x/2L),\ n = 0,1,2,...$$

$$(T_1)_a = \sin((2n+1)\,\pi\, x/2L),\ n = 0,1,2,...$$

i.e. they are symmetric and anti–symmetric odd multiple half wavelength (spatial) modes. Note that the anti–symmetric modes do not vanish at the ends of the wire.

(5) Both the symmetric $(T_2)_s$ and anti–symmetric $(T_2)_a$ modes of Z_2 are also analytic functions of the position, x, along the length of the wire and are of the form

$$(T_2)_s = \cos(n\,\pi\, x/L)\ ,\ n = 0,1,2,....$$

$$(T_2)_a = \sin(n\,\pi\, x/L)\ ,\ n = 0,1,2,....$$

i.e. they are symmetric and anti–symmetric full wave–length (spatial) modes. Note that the symmetric modes do not vanish at the ends of the wire for this case.

(6) The matrix elements of the diagonal matrices z_1 and z_2 are complex; so that radiation damping is included in this representation.

(7) The set of eigenvalues z_1 and the set of eigenvalues z_2 are both doubly degenerate. The eigenvalue $(z_1)_n$ of the eigenvector $(T_1)_s$ is equal to the eigenvalue of the eigenvector $(T_1)_a$ for the same mode number n. Similarly, $(T_2)_s$ and $(T_2)_a$ have equal eigenvalues for the same mode number n.

(8) The resonances of the z_1 eigenvalues occur exactly at odd multiples of the half wavelength for the thin wire (Figure 1). Similarly, the resonances of the z_2 eigenvalues occur exactly at multiples of the full wavelength (Figure 2). These eigenvalues do not exhibit any mode–to–mode coupling. In both Figures 1 and 2, the inverses of the eigenvalues, z_1^{-1} and z_2^{-1}, are presented so that the resonances are easier to identify.

Two aspects of this dual normal mode representation of the impedance matrix require more discussion: (1) the resonant frequencies of the impedance matrix eigenvalues are not equal to the measured values of the resonant frequencies for the thin wire and (2) the $(T_1)_a$ and the $(T_2)_s$ mode shapes do not have zero amplitudes at the ends of the wire. Of the two, the first is the least disturbing since we will show later that the resonant frequencies of the admittance matrix do indeed correspond to the measured values. The physical significance of the impedance matrix eigenvalues is unclear at this time. The second aspect of the dual normal mode representation is more disturbing. One would feel more comfortable if all the mode shapes vanished at the ends of the wire. However, the "unnatural" mode shapes are just the derivatives of the "natural" mode shapes suggesting that they are somehow related to the charge distribution on the wire. Another possible explanation is that one set of modes corresponds to magnetic field modes and the other to electric field modes. This imposed duality is not new in electromagnetics and raises the serious question as to whether a first order time formulation is more natural than a second order time formulation. Perhaps a formulation fashioned after the Hamiltonian theory of classical mechanics [Goldstein (1957)] would shed some light on this subject.

Before concluding our discussion of the impedance matrix, we return once again to our original supposition that the impedance matrix Z_{loop} of a circular wire loop is just some limiting case of a higher order normal mode theory. To support this supposition we note that in the limit as the thin straight wire evolves into a circular loop

$$Z_w = Z_2$$

and the Z_1 contribution to the impedance matrix vanishes. But Z_2 is just equal to Z_{loop} so that for thin wire scatterers our initial supposition is true.

THE DUAL NORMAL MODE REPRESENTATION OF THE ADMITTANCE MATRIX

We have been able to demonstrate up to this point that the impedance matrix for the thin wire can be put into an extremely simple form. A more important question is what about the admittance matrix, Y_w, which is, of course, just the inverse of Z_w? The most desirable behavior would be that the structure of the impedance matrix is form invariant under inversion. This would imply that for the thin wire, Y_w would also be a Toeplitz matrix. From experience, we know that, in general, this is not true.

The next best situation would be that the form of the normal mode decomposition as defined by equations (5),(6),(7) and (12) is preserved under inversion. This would imply that Y_w could be partitioned into the sum of two commuting matrices as before or

$$Y_w(f) = Y_1(f) + Y_2(f) \tag{13}$$

where

$$[Y_1(f_1), Y_1(f_2)] = 0 \tag{14}$$

and

$$[Y_2(f_1), Y_2(f_2)] = 0 \tag{15}$$

for arbitrary f_1 and f_2. We would also require that Y_1 is diagonalizable by the same orthogonal similarity transformation that diagonalized Z_1 and similarly, that Y_2 is diagonalizable by the same similarity transformation that diagonalized Z_2 or

$$y_1(f) = T_1^t Y_1(f) T_1 \tag{16}$$

and

$$y_2(f) = T_2^t Y_2(f) T_2 \tag{17}$$

where $y_1(f)$ and $y_2(f)$ are frequency dependent diagonal matrices and T_1 and T_2 are frequency independent orthogonal matrices as before. If equations (13) through (17) prove to be true, then the admittance matrix $Y_w(f)$ for the thin wire can be written in a compact form given by

$$Y_w(f) = T_1 y_1(f) T_1^t + T_2 y_2(f) T_2^t \tag{18}$$

As was the case for the impedance matrix, the admittance matrix can also be written in terms of two frequency dependent diagonal matrices and two orthogonal frequency independent matrices.

The proof of the identity

$$[T_1 z_1(f) T_1^t + T_2 z_2(f) T_2^t]^{-1} = T_1 y_1(f) T_1^t + T_2 y_2(f) T_2^t \tag{19}$$

turned out to be non–trivial. However, for the decomposition of the impedance matrix as presented in the previous section to be of more than just academic interest, the admittance matrix must also exhibit a similar behavior. Therefore, the proof of the above identity or a similar identity is a very crucial step in the development of this dual normal mode theory.

The first thing of note about the above identity is that

$$y_1(f) = z_1^{-1}(f)$$

and

$$y_2(f) = z_2^{-1}(f)$$

is not a solution. Therefore, in general, y_1 and y_2 are probably non–linear functions of z_1 and z_2.

A review of the literature on inverse matrix theory failed to provide any insight into the proof of the identity given by equation (19). Finally, a numerical demonstration of the validity of the identity was attempted. To do this, we pre–multiply equation (18) by T_1^t and post–multiply by T_1 which results in the equation

$$y_1(f) + T_1^t T_2 y_2(f) T_2^t T_1 = T_1^t Y_w(f) T_1 \tag{20}$$

Next, we pre–multiply equation (18) by T_2^t and post–multiply by T_2 which results in the equation

$$T_2^t T_1 y_1(f) T_1^t T_2 + y_2(f) = T_2^t Y_w(f) T_2 \tag{21}$$

First of all we note that $S^t = T_2^t T_1$ and $S = T_1^t T_2$ are both frequency independent orthogonal matrices with $S^t S = S S^t = I$ (the identity matrix). Next, we note that equations (20) and (21) yield $2N^2$ equations for the $2N$ unknowns y_1 and y_2. Using only the $2N$ equations provided by the diagonal elements of the matrices defined by equations (20) and (21), y_1 and y_2 can be determined from solutions of the equation

$$Hy(f) = h(f) \qquad (22)$$

where y(f) and h(f) are 2Nx1 column vectors and H is a 2Nx2N frequency independent matrix. The first N elements of y(f) correspond to the N diagonal elements of $y_1(f)$ and the second N elements of y(f) correspond to the N diagonal elements of $y_2(f)$. The first N elements of h(f) correspond to the N diagonal elements of the matrix $T_1^tY_w(f)T_1$ and the second N elements of h(f) correspond to the N diagonal elements of $T_2^tY_w(f)T_2$. If H is partitioned into the four NxN matrices: $H_{11}, H_{12}, H_{21}, H_{22}$; then H_{11} and H_{22} are equal to the NxN identity matrix I, or

$$H_{11} = H_{22} = I,$$

the elements of H_{12} are given by

$$(H_{12})_{ij} = (S_{ij})^2$$

and the elements of H_{21} are given by

$$(H_{21})_{ij} = (S_{ji})^2$$

where

$$S_{ij} = (T_1^tT_2)_{ij}.$$

Equation (22) was solved numerically over a frequency range corresponding to a wire length–to–wavelength ratio of 0.05 to 2.0. The impedance matrix, $Z_w(f)$, was derived from a hybrid finite difference/method of moments technique using pulse expansion functions with point matching. The wire was divided into 20 segments and the wire radius–to–length ratio was 0.005. Since H is independent of frequency, the resulting 40x40 matrix only had to be inverted once. The values of $y_1(f)$ and $y_2(f)$ obtained from equation (22) were inserted into equation (18) and the resulting values obtained for $Y_w(f)$ were then compared to the values $Y_w(f)$ obtained by directly inverting $Z_w(f)$. The results for 6 elements of the admittance matrix are shown in Figures 3 through 8. Comparisons for other matrix elements showed similar agreement.

Although the comparison of the results of the two calculations was excellent, they still were not exact. This could either be attributed to numerical round–off error since the calculations were performed on a PC AT computer using single precision or it could be attributed to small contributions to the admittance matrix that were not included in equation (18). Another literature search on the subject of inverse matrix theory failed to provide any new insight. Then it was discovered that another matrix besides the identity matrix commutes with both $Z_1(f)$ and $Z_2(f)$ of equation (5), therefore, it is also diagonalizable by both the orthogonal similarity transformations defined by T_1 and T_2 of equations (8) and (9). This matrix is the cross identity matrix, E, i.e. the major cross diagonal elements of E are equal to one and all other elements are zero. With the aid of this matrix, one can then show that if a matrix Z can be partitioned into the sum of two commuting matrices as defined by equations (5),(6) and (7), then Z^2 can also be partitioned into the sum of two matrices (but not the same two matrices) that have the same properties. If this is true for Z^2, it is also true for Z^3 and all higher powers of Z (the proof for a 4x4 matrix is shown in Appendix B). Using the Cayley–Hamilton theorem [Wilson, Decius and Cross (1955)], the inverse of the NxN matrix, Z_w, can be written in the form

$$Z_w^{-1} = Y_w = -[C_{N-1} + C_{N-2}Z_w + C_{N-3}Z_w^2 + \dots$$

$$\dots + C_1 Z_w^{N-2} + Z_w^{N-1}]/C_N \tag{23}$$

and therefore, equations (13) through (17) follow and we have proved the identity given by equation (19). In equation (23), all of the C's are scalars and they are the coefficients of the characteristic equation for Z_w; for example, C_1 is the negative of the trace of Z_w and C_N is the negative of the determinant of Z_w. Equation (18) also follows and we have succeeded in demonstrating that the admittance matrix can be written in the very simple form

$$Y_w(f) = T_1 y_1(f) T_1^t + T_2 y_2(f) T_2^t \tag{18}$$

which only requires two frequency dependent diagonal matrices and two frequency independent orthogonal real matrices as compared to the 2N frequency dependent diagonal matrices and the 2N frequency independent non–orthogonal complex matrices that result from the SEM formulation.

The eigenvalues, $y_1(f)$ and $y_2(f)$, of the two admittance matrices $Y_1(f)$ and $Y_2(f)$ were calculated over the frequency range corresponding to a wire length to wavelength ratio of 0.05 to 2.0. The calculations were performed for a 20 segment wire, again using a hybrid finite difference/method of moments technique with pulse expansion functions and point matching. Results of the calculations are presented in Figures 9 through 12. Some of the interesting behavior exhibited by these eigenvalues is:

(1) The response resonances of these eigenvalues occur at the same frequencies as observed in measured data, i.e. they are no longer "exact" multiples of half and full wavelengths as was the case for the eigenvalues of the impedance matrix.

(2) The eigenvalues (Figures 9 and 11) associated with the symmetric mode shapes exhibit odd multiple of half wavelength resonances while the eigenvalues (Figures 10 and 12) associated with the anti–symmetric mode shapes exhibit multiple of full wavelength resonances. Remember that this was not true for the impedance matrix eigenvalues.

(3) While the impedance matrix eigenvalues did not exhibit any mode–to–mode coupling, the eigenvalues of the admittance matrix exhibit strong mode–to–mode coupling behavior for some of the eigenvalues.

(4) The admittance matrix appears to exhibit a very high degree of degeneracy (or "near" degeneracies) over the frequency range for which the eigenvalues were calculated. This degeneracy persists even for the phase of the eigenvalues (Figure 9.b) with similar results for the other set of eigenvalue phases (not shown).

It will be interesting to see if the redundancy which manifests itself through the degeneracies of the admittance matrix eigenvalues persists over a higher frequency range. The thin straight wire is only a two parameter problem, namely length to wavelength ratio and length to radius ratio, therefore one would expect considerable redundancy in its response characterization over a considerable frequency range.

One of the features that will require more investigation is the strong mode–to–mode coupling exhibited by the symmetric modes (Figures 9 and 11) at frequencies near the first resonance (approximately half wavelength) of the thin wire. It appears that all of the symmetric modes contribute significantly to the first resonance response. For frequencies near the second symmetric resonance (Figures 9 and 11), the nearest neighbor modes, modes 0 and 2, are coupled more strongly than the higher order modes. For the anti–symmetric modes (Figures 10 and 12), the modal coupling is also the strongest for the nearest neighbor modes.

POTENTIAL APPLICATIONS

For many years, normal mode techniques have played a powerful role in the analysis of the dynamic response of complex structural systems and their environments. This role is not limited to numerical response predictions but has included test definition, data analysis and system identification. These normal mode techniques provide a convenient bridge between model predictions and test results which is always an important consideration in any area of physics. Although, there is no guarantee that normal mode techniques will display a similar robust character when applied to the exterior EM interaction problem, there is also no reason, at this time, to assume otherwise.

The first and most obvious benefit of the technique would result if it provides better understanding and insight into the physics and the nature of EM coupling problems. This could potentially lead to the development of good self–consistent approximate models and to simpler and more meaningful measurement techniques.

From strictly a computational point of view, there are several possibilities. First a significant reduction in the number of unknowns can usually be achieved by making the transformation to normal coordinates. For example, if the expansion functions used in the discretization require 10 segments per wavelength from accuracy considerations, then only the first N/10 modal coordinates need to be retained in the calculations since the higher order mode contributions will be in error. Also, it maybe possible to partition a complex scatterer into several distinct regions such that the total system can be reconstructed by using the modal coordinates of each region as the expansion functions. Another possibility includes reducing matrix fill time for applications that require the prediction of responses over a wide frequency range. Also, it may be possible to treat the mode density as a continuum (rather than discrete) which potentially could provide us with a method for increasing the upper frequency limits for the numerical techniques currently in use.

One area that has a great practical potential is the whole field of EM measurements. If it can be shown that the eigenvalues of the admittance matrix can be directly or easily related to measurements, then the technique will provide a simple format for categorizing the response of radiating structures. This will be useful as a tool for retaining information about general classes of radiating objects, for extrapolating near field measurements to far field responses and possibly for identifying objects from far field measurements. However, for the last application to be feasible, algorithms that relate the impedance matrix eigenvalues to the admittance matrix eigenvalues will be required, since the impedance matrix "footprint" is significantly simpler than that of the admittance matrix.

SUMMARY

We have demonstrated that both the impedance and admittance matrices for a straight thin wire can be put into a simple form by using a dual normal mode formulation. The mode shapes associated with the normal modes are real and are neither functions of time nor frequency. They can be represented numerically by real orthogonal matrices. The dynamic or transient part of the interaction can be characterized by diagonal matrices which are complex numbers (in the frequency domain) and are functions of either time or frequency. These elements of the diagonal matrices could be referred to as the modal frequencies. However, one must keep in mind that there is no one–to–one correspondence between the modal frequencies associated with the impedance matrix and the modal frequencies associated with the admittance matrix. The impedance matrix modal frequencies have only one resonant frequency but that frequency does not coincide with measured resonant frequencies. The resonances of the admittance matrix modal frequencies do coincide with the measured resonant frequencies but each of these modal frequencies possess multiple resonances. Maybe it would be less confusing to refer to the impedance matrix modal frequencies as the system frequencies and the admittance matrix modal frequencies as the transfer frequencies.

In many respects, the dual normal mode representation is much simpler than the representation provided by the Singularity Expansion Method. However, the transfer frequencies (eigenvalues of the admittance matrix) are no longer one–parameter rational functions of the frequency. The functional behavior of the transfer frequencies needs to be determined.

Clearly, much work on the dual normal mode representation needs to be done. Issues regarding its extension to more complex scatterers need to be investigated. The physical significance of the system frequencies (eigenvalues of the impedance matrix) and the mode shapes that do not satisfy the boundary conditions at the end of the wire needs to be determined. The relationship between the transfer frequencies and measured data must be established. However, if it can be demonstrated that the dual normal mode representation simply and efficiently bridges the gap between models and measurements, it has the potential of providing us with a very powerful tool applicable to almost every facet of the EM interaction and scattering problem.

REFERENCES:

Baum, C. E., "On the Singularity Expansion Method for the Solution of Electromagnetic Interaction Problems," Interaction Note 88, Air Force Weapons Laboratory, Albuquerque, NM, December 1971.

Richardson, M. and R. Potter, "Identification of the Modal Properties of an Elastic Structure from Measured Transfer Function Data," Presented at the 20th International Instrumentation Symposium, Instrument Society of America, Albuquerque, NM, May 1974 (pp. 239).

Cordaro, J. T. and W. A. Davis, "Time–Domain Techniques in the Singularity Expansion Method," IEEE Transactions on Antennas and Propagation, Vol. AP–29, No. 3, May 1981.

Caughey, T.K. and M.E.J. O'Kelly, "Classical Normal Modes in Damped Linear Systems," Journal of Applied Mechanics, September 1965.

Arfken, G., Mathematical Methods for Physicists, Academic Press, New York, NY, 1966.

Goldstein, H., Classical Mechanics, Addison–Wesley, Reading, MA, 1957.

Wilson, E. B. , Decius, J. C. and Cross, P. C., Molecular Vibrations, The Theory of Infrared and Raman Vibrational Spectra, McGraw–Hill, New York, NY, 1955.

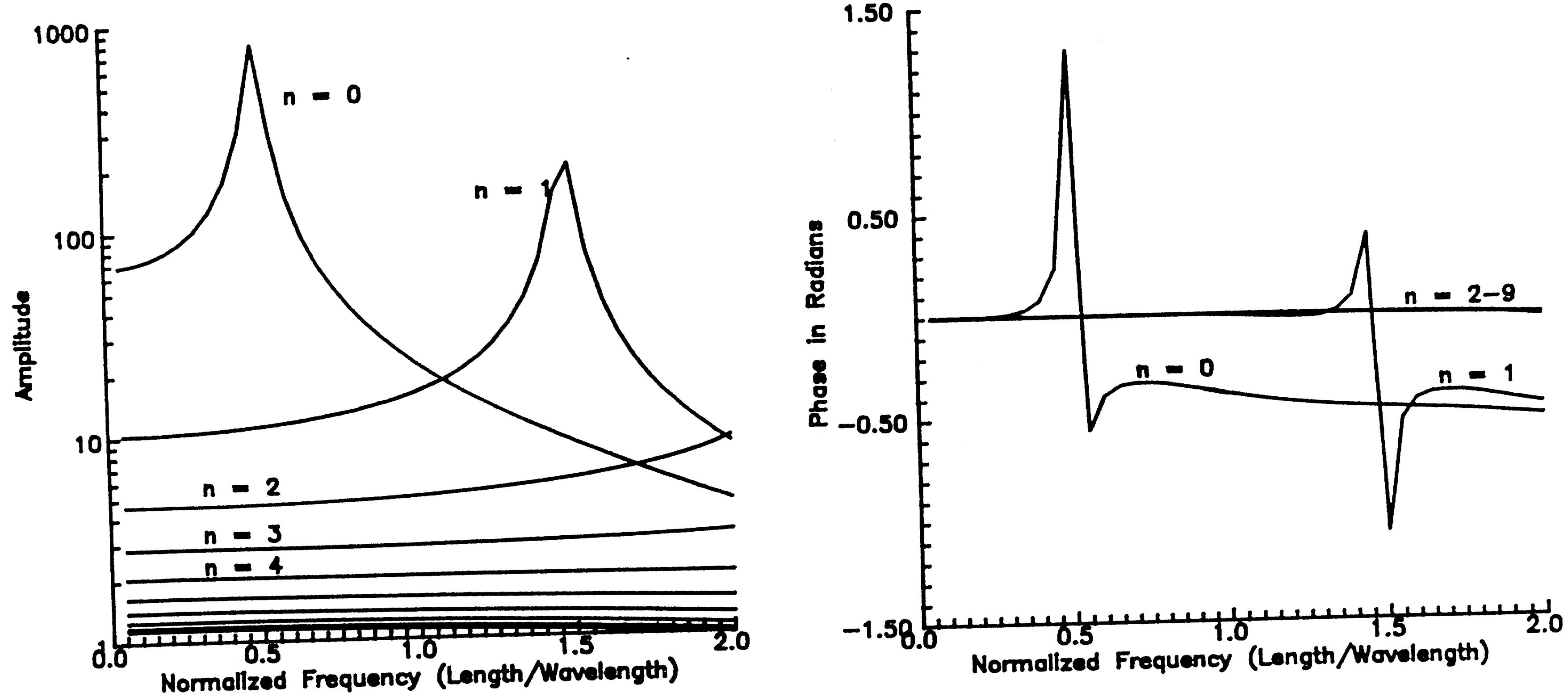

Figure 1. The inverse of the first ten eigenvalues of the Z_1 impedance matrix.

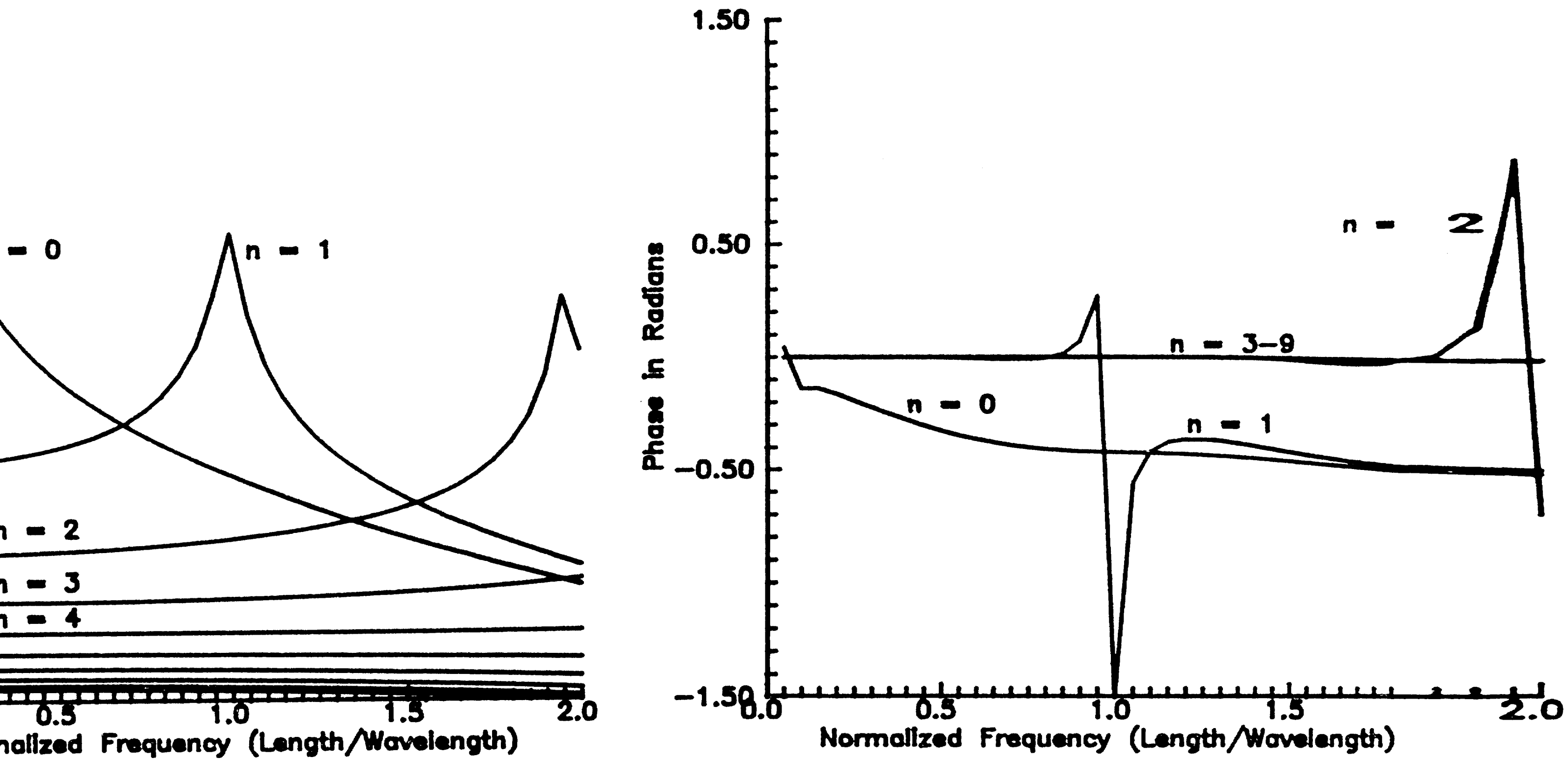

Figure 2. The inverse of the first ten eigenvalues of the Z_2 impedance matrix.

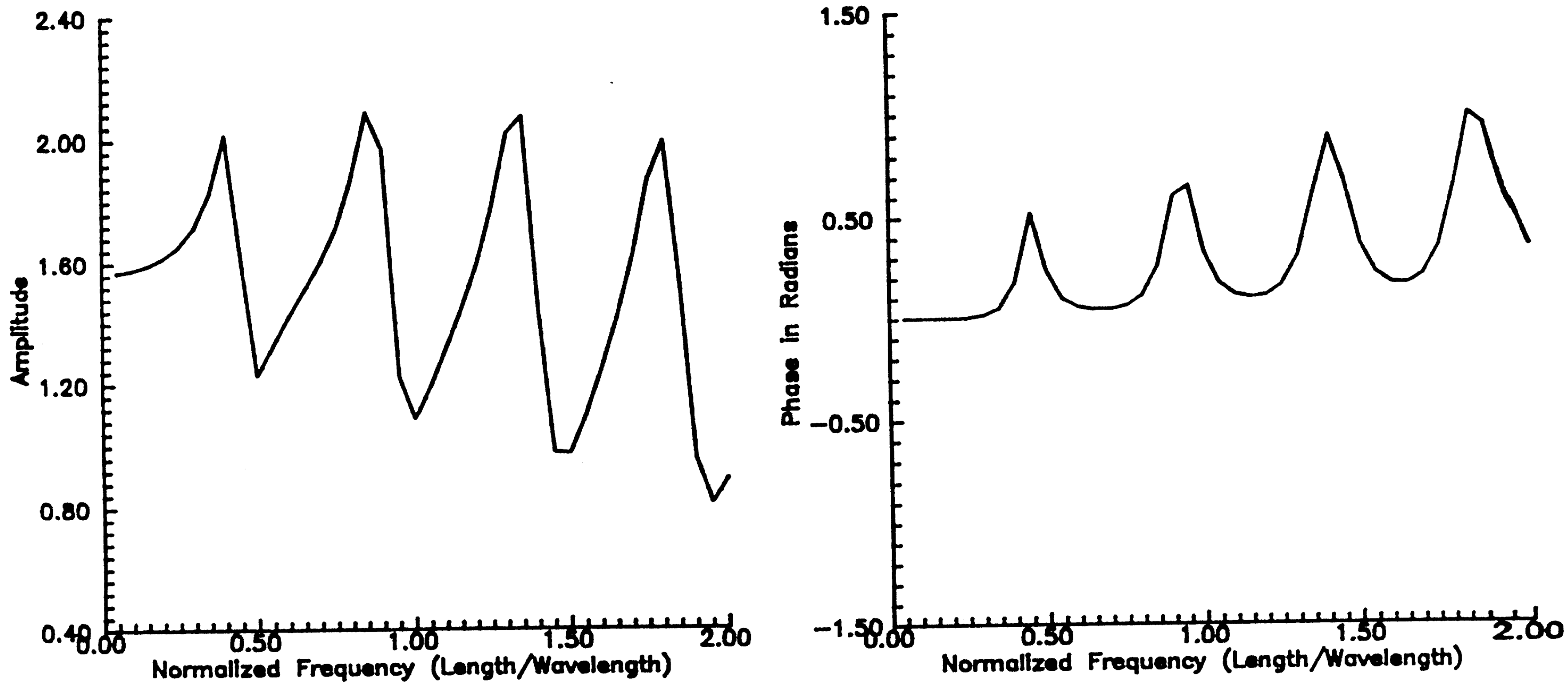

Figure 3. Comparison of the inverse method (–) vs. eigenvalue method (– – –) for the $Y_{1,1}$ element for the admittance matrix.

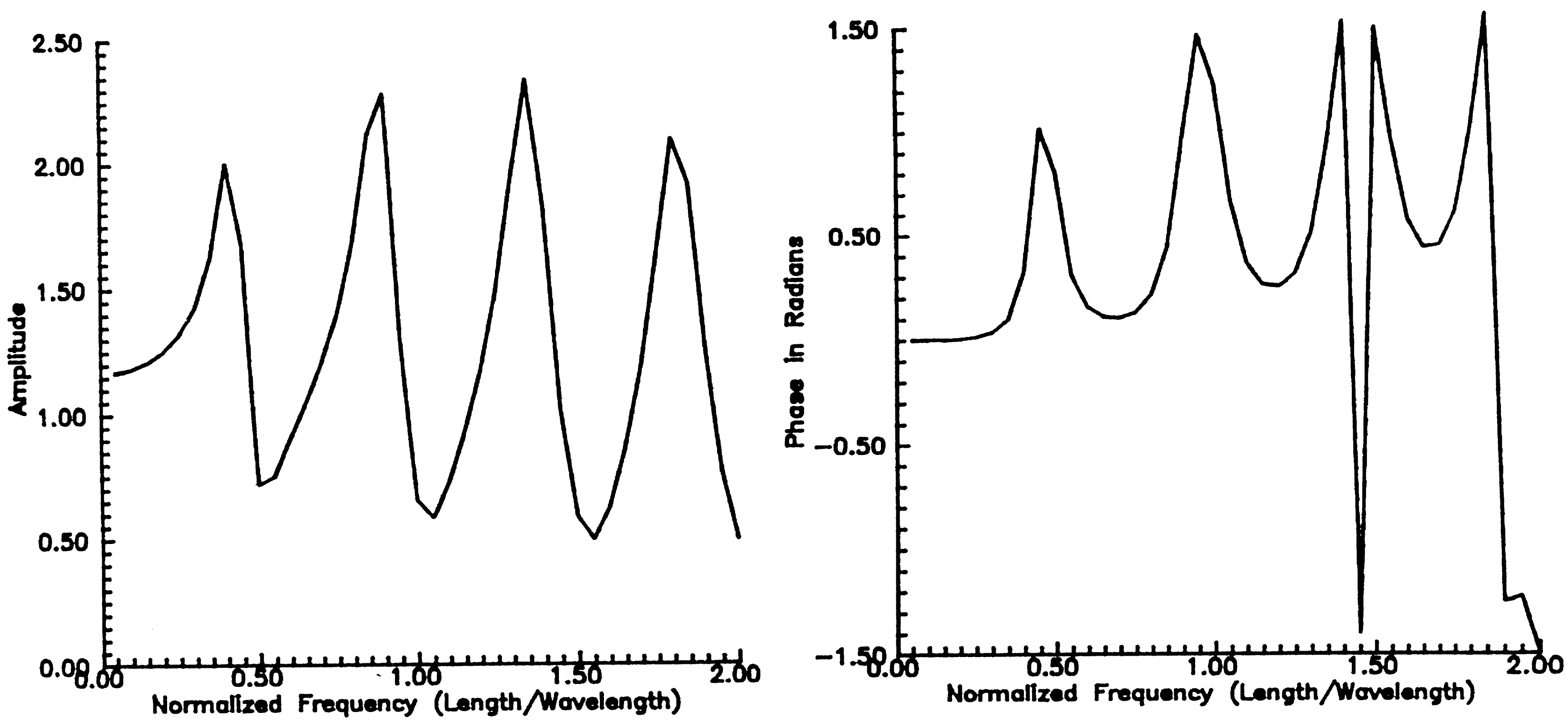

Figure 4. Comparison of the inverse method (–) vs. the eigenvalue method (– – –) for the $Y_{1,2}$ element of the admittance matrix.

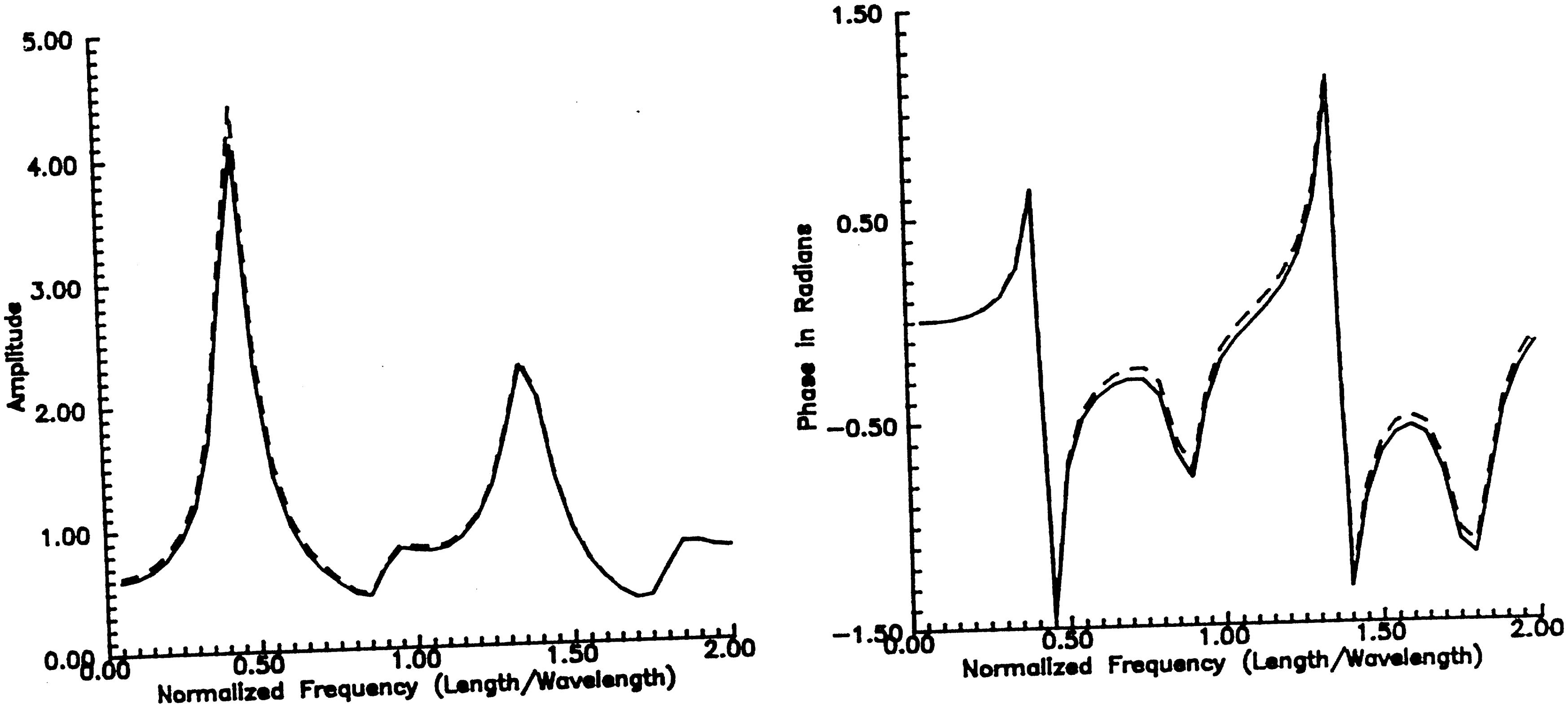

Figure 5. Comparison of the inverse method (–) vs. the eigenvalue method (– – –) for the $Y_{1,\,10}$ element of the admittance matrix.

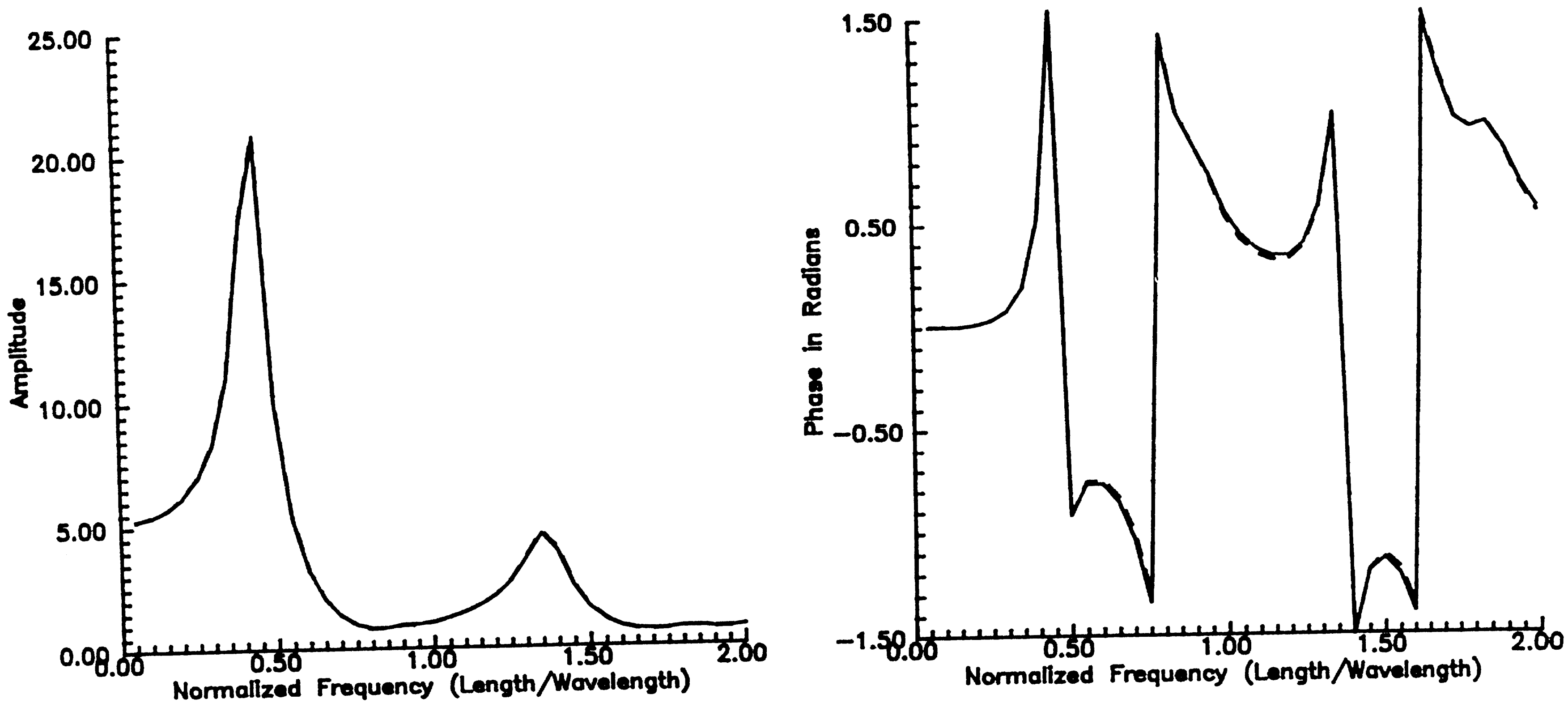

Figure 6. Comparison of the inverse method (–) vs. the eigenvalue method (– – –) for the $Y_{10,\,10}$ element of the admittance matrix.

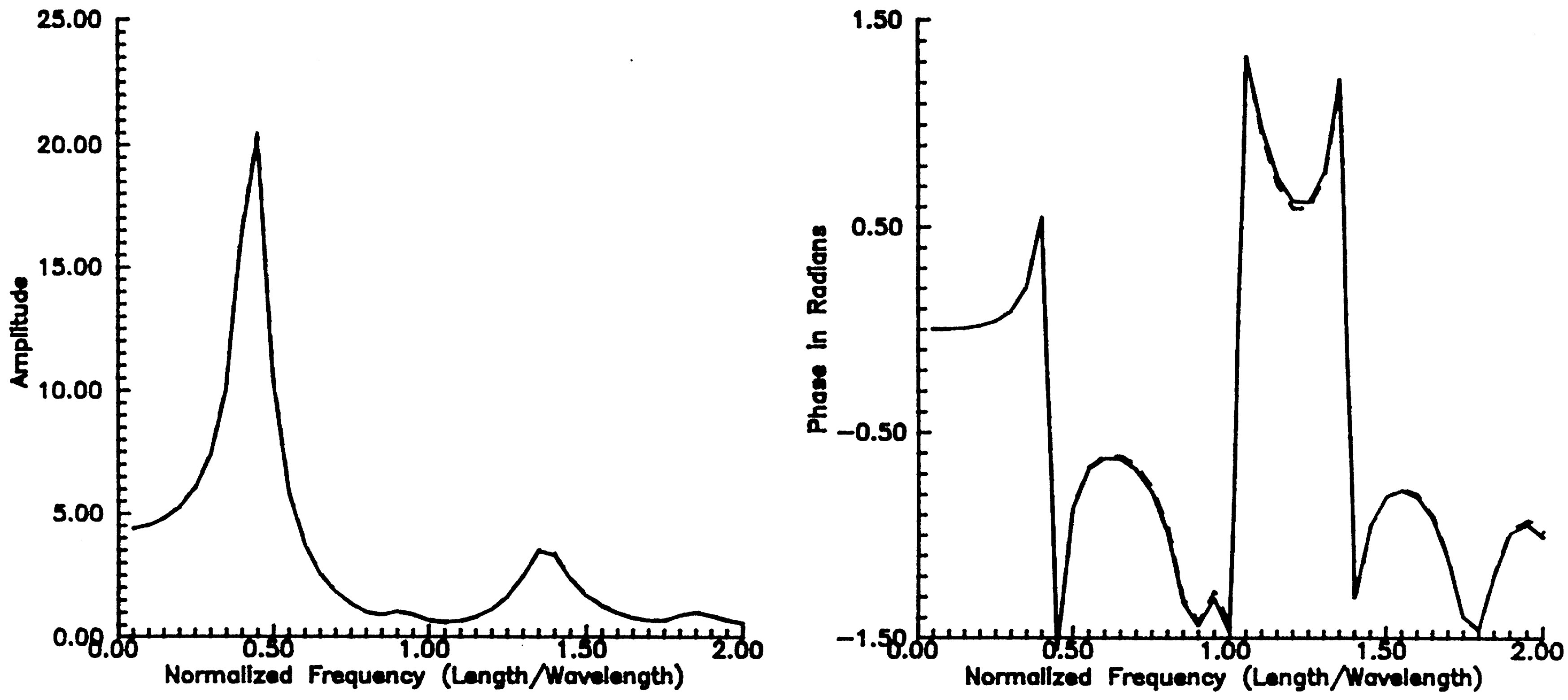

Figure 7. Comparison of the inverse method (–) vs. the eigenvalue method (– – –) for the $Y_{10,\,9}$ element of the admittance matrix.

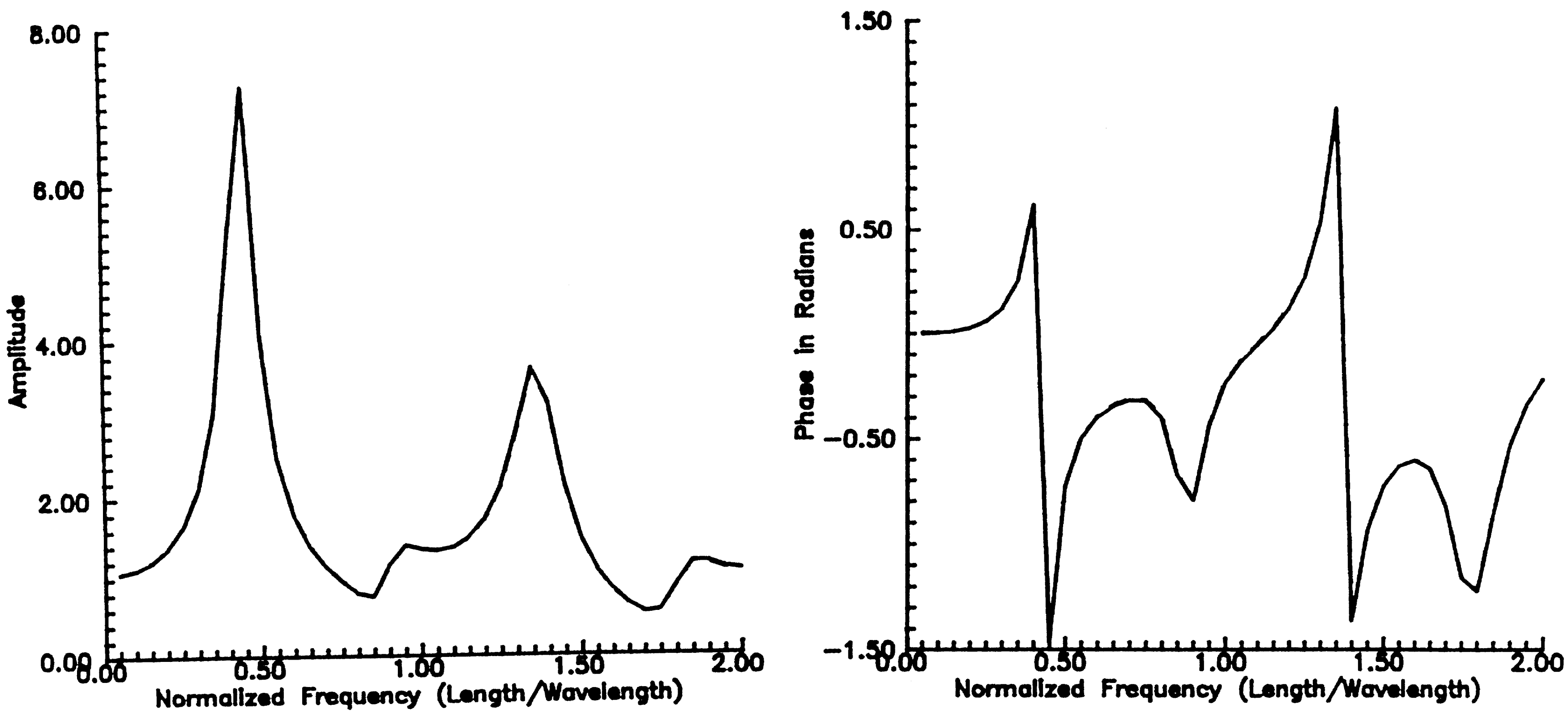

Figure 8. Comparison of the inverse method (–) vs. the eigenvalue method (– – –) for the $Y_{10,\,2}$ element of the admittance matrix.

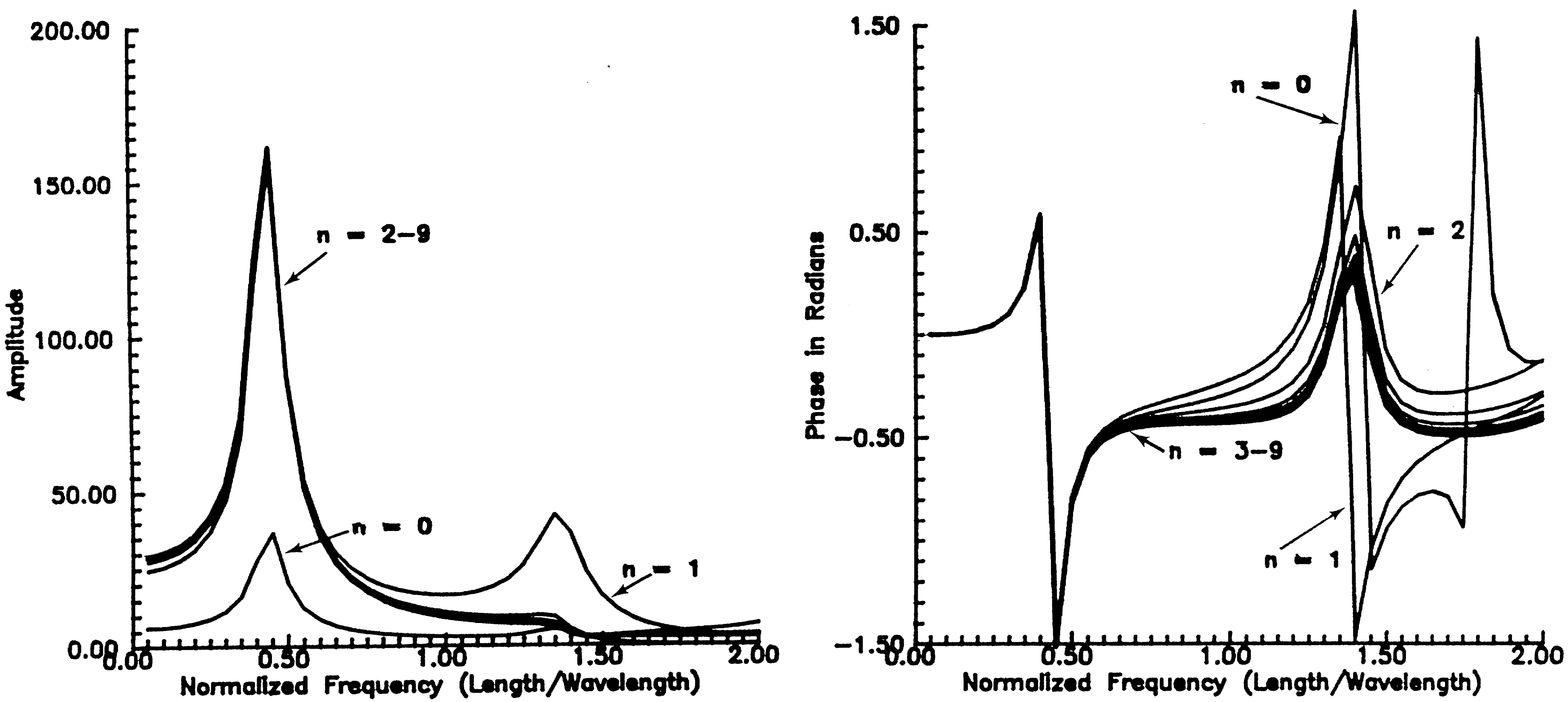

Figure 9. The first ten eigenvalues of the Y_1 matrix.

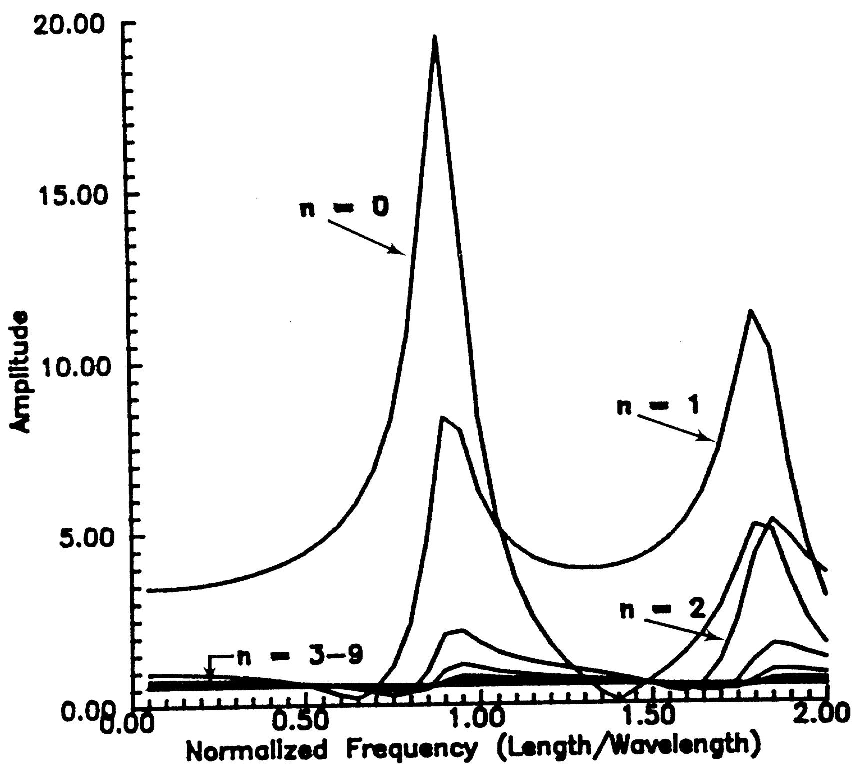

Figure 10. The amplitudes of the second ten eigenvalues for the Y_1 matrix.

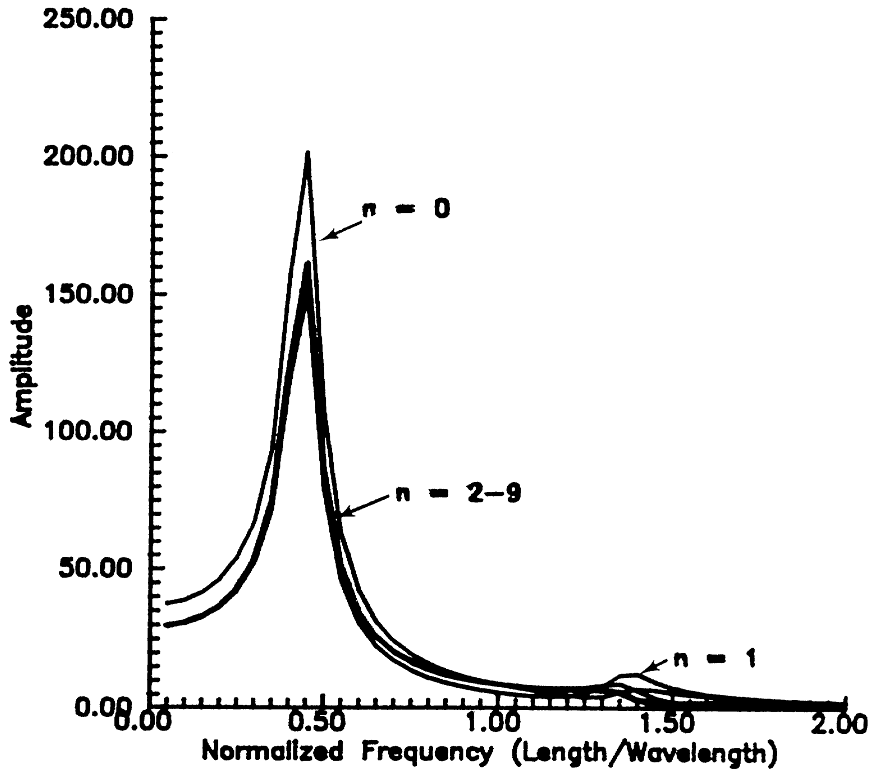

Figure 11. The amplitude of the first ten eigenvalues for the Y_2 matrix.

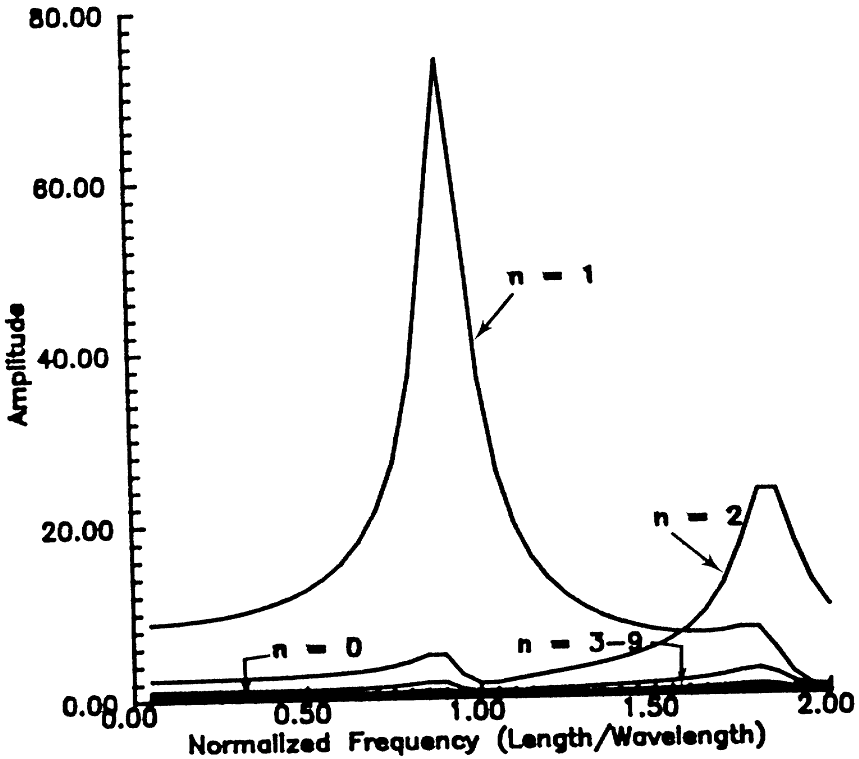

Figure 12. The amplitude of the second ten eigenvalues for the Y_2 matrix.

APPENDIX A

To prove that the impedance matrix, Z_w, can be partitioned into the sum of two commuting matrices as defined by equations (5), (6) and (7), we begin by writing Z_w in the form:

$$Z_w(f) = \sum_{n=0}^{N-1} \alpha_n(f)\, \phi_n \tag{A.1}$$

where the α's are just frequency dependent scalars and the ϕ's are frequency independent NxN matrices of the form

$$\phi_0 = I \text{ (identity matrix)},$$

$$\phi_1 = \begin{bmatrix} 0\;1\;0\;0 \cdot\cdot\cdot 0\;0 \\ 1\;0\;1\;0 \cdot\cdot\cdot 0\;0 \\ 0\;1\;0\;1 \cdot\cdot\cdot 0\;0 \\ \cdot\;\cdot\;\cdot\;\cdot\;\cdot\;\cdot\;\cdot\;\cdot\;\cdot\;\cdot \\ \cdot\;\cdot\;\cdot\;\cdot\;\cdot\;\cdot\;\cdot\;\cdot\;\cdot\;\cdot \\ \cdot\;\cdot\;\cdot\;\cdot\;\cdot\;\cdot\;\cdot\;\cdot\;\cdot\;\cdot \\ 0\;0 \cdot\cdot\cdot 1\;0\;1\;0 \\ 0\;0 \cdot\cdot\cdot 0\;1\;0\;1 \\ 0\;0 \cdot\cdot\cdot 0\;0\;1\;0 \end{bmatrix}$$

$$\phi_2 = \begin{bmatrix} 0\;0\;1\;0\;0 \cdot\cdot 0\;0 \\ 0\;0\;0\;1\;0 \cdot\cdot 0\;0 \\ 1\;0\;0\;0\;1 \cdot\cdot 0\;0 \\ \cdot\;\cdot\;\cdot\;\cdot\;\cdot\;\cdot\;\cdot\;\cdot\;\cdot\;\cdot \\ \cdot\;\cdot\;\cdot\;\cdot\;\cdot\;\cdot\;\cdot\;\cdot\;\cdot\;\cdot \\ \cdot\;\cdot\;\cdot\;\cdot\;\cdot\;\cdot\;\cdot\;\cdot\;\cdot\;\cdot \\ 0\;0 \cdot\cdot 1\;0\;0\;0\;1 \\ 0\;0 \cdot\cdot 0\;1\;0\;0\;0 \\ 0\;0 \cdot\cdot 0\;0\;1\;0\;0 \end{bmatrix}$$

$$\vdots$$

$$\phi_{N-2} = \begin{bmatrix} 0 & 0 & \cdots & 0 & 1 & 0 \\ 0 & 0 & \cdots & 0 & 0 & 1 \\ \vdots & & & & & \vdots \\ 1 & 0 & 0 & \cdots & 0 & 0 \\ 0 & 1 & 0 & \cdots & 0 & 0 \end{bmatrix}$$

$$\phi_{N-1} = \begin{bmatrix} 0 & 0 & \cdots & 0 & 1 \\ 0 & 0 & \cdots & 0 & 0 \\ \vdots & & & & \vdots \\ 0 & 0 & \cdots & 0 & 0 \\ 1 & 0 & \cdots & 0 & 0 \end{bmatrix}$$

$$\phi_N = 0 \text{ (null matrix)}.$$

The ϕ's do not commute or

$$[\phi_n, \phi_m] = \phi_n\phi_m - \phi_m\phi_n \neq 0 \tag{A.2}$$

unless $n = m$ or $n = 0$ or $n = N$ or $m = 0$ or $m = N$. If we define two new sets of matrices, $\bar{\chi}_n$ and χ_n, by the relationships

$$\chi_n = \phi_n - \phi_{N-n} \tag{A.3}$$

and

$$\bar{\chi}_n = \phi_n + \phi_{N-n} \tag{A.4}$$

and add equations (A.3)and (A.4) we can write ϕ_n in terms of these new matrices or

$$\phi_n = (\chi_n + \bar{\chi}_n)/2. \tag{A.5}$$

substituting equation (A.5) into equation (A.1) yields

$$Z_w(f) = {}^1/_2 \sum_{n=0}^{N-1} \alpha_n (f)\, \chi_n + {}^1/_2 \sum_{n=0}^{N-1} \alpha_n (f)\, \bar{\chi}_n \tag{A.6}$$

and by defining

$$Z_1(f) = {}^1/_2 \sum_{n=0}^{N-1} \alpha_n(f)\, \chi_n$$

and

$$Z_2(f) = {}^1/_2 \sum_{n=0}^{N-1} \alpha_n(f)\, \tilde{\chi}_n$$

equation (5) follows or

$$Z_w(f) = Z_1(f) + Z_2(f) \tag{5}$$

But

$$[\chi_n, \chi_m] = 0$$

and

$$[\tilde{\chi}_n, \tilde{\chi}_m] = 0$$

for all n and m. Therefore, equations (6) and (7) follow or

$$[Z_1(f_1), Z_1(f_2)] = 0 \tag{6}$$

and

$$[Z_2(f_1), Z_2(f_2)] = 0 \tag{7}$$

for all f_1 and f_2. One possible generalization of equation (A.5) to arbitrarily shaped wires was suggested by J. W.Williams [private communication]. This generalized form is given by

$$\phi_n = g\, \chi_n + (1-g)\, \tilde{\chi}_n \tag{A.7}$$

where g is now a geometric shape factor. For a straight wire, $g = {}^1/_2$ and equation (A.5) follows. For a wire loop, $g = 0$ and Z_w reduces to

$$Z_w(f) = \sum_{n=0}^{N-1} \alpha_n(f)\, \tilde{\chi}_n \tag{A.8}$$

which is the form of the impedance matrix for a wire loop.

APPENDIX B

To show that the admittance matrix, Y_w, can be written in the form

$$Y_w = T_1 y_1 T_1^t + T_2 y_2 T_2^t \tag{18}$$

for the case of a 4x4 impedance matrix, we begin by writing the normalized impedance matrix, Z, given by

$$\begin{aligned} Z &= Z_w/\alpha_0 \\ &= I_4 + X_4 \end{aligned} \tag{B.1}$$

where

$$X_4 = \beta_1\phi_1 + \beta_2\phi_2 + \beta_3\phi_3,$$

$$\beta_1 = \alpha_1/\alpha_0, \ \beta_2 = \alpha_2/\alpha_0, \ \beta_3 = \alpha_3/\alpha_0,$$

$$I_4 = \begin{bmatrix} 1&0&0&0 \\ 0&1&0&0 \\ 0&0&1&0 \\ 0&0&0&1 \end{bmatrix} \qquad \phi_1 = \begin{bmatrix} 0&1&0&0 \\ 1&0&1&0 \\ 0&1&0&1 \\ 0&0&1&0 \end{bmatrix}$$

$$\phi_2 = \begin{bmatrix} 0&0&1&0 \\ 0&0&0&1 \\ 1&0&0&0 \\ 0&1&0&0 \end{bmatrix} \qquad \phi_3 = \begin{bmatrix} 0&0&0&1 \\ 0&0&0&0 \\ 0&0&0&0 \\ 1&0&0&0 \end{bmatrix}$$

and the α's are the frequency dependent coefficients defined by equation (A.1) of Appendix A. The Cayley–Hamilton theorem states that a matrix satisfies its own characteristic equation or

$$Z^4 + C_1 Z^3 + C_2 Z^2 + C_3 Z + C_4 = 0 \tag{B.2}$$

where the C's are scalars. Therefore,the inverse of Z, $Y = Z^{-1}$, is given by

$$\begin{aligned} Y &= -[C_3 + C_2 Z + C_1 Z_2 + Z^3]/C_4 \\ &= -[(I_4+C_1+C_2+C_3) + (C_2+2C_1+3)X_4 + (C_1+3)X_4^2 + X_4^3]/C_4 \end{aligned} \tag{B.3}$$

We have already shown in Appendix A that the first two terms of equation (A.3) can be reduced to the desired form; therefore we will address only the X_4^2 and X_4^3 terms.

$\underline{X_4^2}$:

Expanding X_4^2 in terms of its primitive matrices we have

$$X_4^2 = \beta_1^2\,\phi_1^2 + \beta_2^2\,\phi_2^2 + \beta_3^2\,\phi_3^2 + \beta_1\,\beta_2\,(\phi_1\phi_2 + \phi_2\phi_1)$$
$$\beta_1\,\beta_3\,(\phi_1\phi_3 + \phi_3\phi_1) + \beta_2\beta_3\,(\phi_2\phi_3 + \phi_3\phi_2) \tag{B.4}$$

with

$$\phi_1^2 = 2I_4 - E_4 + \phi_2$$

$$\phi_2^2 = I_4$$

$$\phi_3^2 = E_4\phi_3$$

$$\phi_1\phi_2 + \phi_2\phi_1 = 2E_4 + 2E_4\phi_2$$

$$\phi_1\phi_3 + \phi_3\phi_1 = \phi_2$$

$$\phi_2\phi_3 + \phi_3\phi_2 = E_4\phi_2$$

where

$$E_4 = \begin{bmatrix} 0 & 0 & 0 & 1 \\ 0 & 0 & 1 & 0 \\ 0 & 1 & 0 & 0 \\ 1 & 0 & 0 & 0 \end{bmatrix}.$$

$\underline{X_4^3}$:

Similarly, expanding X_4^3 in terms of its primitive matrices we have

$$\begin{aligned} X_4^3 \quad &= \beta_1^3\phi_1^3 + \beta_2^3\phi_2^3 + \beta_3^2\phi_3^2 + \beta_1\beta_2^2\,(\phi_1\phi_2^2 + \phi_2\phi_1\phi_2 + \phi_2^2\phi_1) \\ &+ \beta_1\beta_3^2(\phi_1\phi_3^2 + \phi_3\phi_1\phi_3 + \phi_3^2\phi_1) + \beta_1^2\beta_2(\phi_2\phi_1^2 + \phi_1\phi_2\phi_1 + \phi_1^2\phi_2) \\ &+ \beta_2\beta_3^2(\phi_2\phi_3^2 + \phi_3\phi_2\phi_3 + \phi_3^2\phi_2) + \beta_1^2\beta_3(\phi_3\phi_1^2 + \phi_1\phi_3\phi_1 + \phi_1^2\phi_3) \\ &+ \beta_2^2\beta_3(\phi_3\phi_2^2 + \phi_2\phi_3\phi_2 + \phi_2^3\phi_3) \\ &+ \beta_1\beta_2\beta_3(\phi_1\phi_2\phi_3 + \phi_1\phi_3\phi_2 + \phi_2\phi_1\phi_3 + \phi_2\phi_3\phi_1 + \phi_3\phi_1\phi_2 + \phi_3\phi_2\phi_1) \end{aligned} \tag{B.5}$$

with

$$\phi_1^3 = 2\phi_1 + E_4$$

$$\phi_2^3 = \phi_2$$

$$\phi_3^3 = \phi_3$$

$$\phi_1\phi_2^3 + \phi_2\phi_1\phi_2 + \phi_2^2\phi_1 = \phi_1 + E_4 + 2E_4\phi_2$$

$$\phi_1\phi_3^2 + \phi_3\phi_1\phi_3 + \phi_3^2\phi_1 = E_4\phi_2$$

$$\phi_2\phi_1^2 + \phi_1\phi_2\phi_1 + \phi_1^2\phi_2 = 4I_4 + 4\phi_2 - 2E_4\phi_3$$

$$\phi_2\phi_3^2 + \phi_3\phi_2\phi_3 + \phi_3^2\phi_2 = \phi_2$$

$$\phi_3\phi_1^2 + \phi_1\phi_3\phi_1 + \phi_1^2\phi_3 = \phi_1 + 2\phi_3$$

$$\phi_3\phi_2^2 + \phi_2\phi_3\phi_2 + \phi_2^2\phi_3 = \phi_3 + E_4$$

$$\phi_1\phi_2\phi_3 + \phi_1\phi_3\phi_2 + \phi_2\phi_1\phi_3 + \phi_2\phi_3\phi_1 + \phi_3\phi_1\phi_2 + \phi_3\phi_2\phi_1 = 2I_4 + \phi_2 + 2E_4\phi_3.$$

Collecting terms, equation (B.3) can now be written in the form

$$Y = \sum_{n=0}^{3} \Gamma_n(f;I_4,E_4)\phi_n. \tag{B.6}$$

But since

$$[I_4,\phi_n] = 0$$

and

$$[E_4,\phi_n] = 0$$

for all n, the results of Appendix A also hold for equation (B.6) and equation (18) follows:

$$Y_w = T_1y_1T_1^t + T_2y_2T_2^t \tag{18}$$